Available online at www.sciencedirect.com
SCIENCE DIRECT®
International Journal of Heat and Mass Transfer 48 (2005) 3485–3492
International Journal of HEAT and MASS TRANSFER
www.elsevier.com/locate/ijhmt

A scaling analysis to characterize thermomagnetic convection

Achintya Mukhopadhyay [a], Ranjan Ganguly [b,c], Swarnendu Sen [a], Ishwar K. Puri [d,*]

[a] Department of Mechanical Engineering, Jadavpur University, Kolkata 700 032, India
[b] Department of Mechanical and Industrial Engineering, University of Illinois at Chicago, Chicago, IL 60607, USA
[c] Department of Power Engineering, Jadavpur University, Kolkata 700 032, India
[d] Department of Engineering Science and Mechanics, Virginia Polytechnic Institute and State University, Blacksburg, VA 24061, USA

Received 28 October 2004; received in revised form 25 March 2005
Available online 17 May 2005

Abstract

Thermomagnetic convection is characterized using scaling arguments. We consider a square enclosure filled with a ferrofluid that is under the influence of an external magnetic field created by a line dipole. The height-averaged Nusselt number scales with the magnetic Rayleigh number as $Nu \sim Ra_m^{0.25}$. This result is in excellent agreement with predictions obtained from detailed numerical simulations. Use of the Langevin equation of ferrofluid magnetization identifies an optimum enclosure height for which the Nusselt number reaches a maximum value for a given line dipole strength.

1. Introduction

Thermogravitational or free convection occurs under many circumstances and is used in numerous applications. However, its effectiveness greatly diminishes at small length scales as other effects become dominant. Buoyancy-induced convection ceases to be effective in reduced gravity, e.g., in spacecraft. Thermomagnetic convection is a feasible method to augment or suppress free convection for small length scale applications or in hypogravity [1,2], but it is not yet fully characterized. A thorough understanding of the relation between an applied magnetic field and the resulting heat transfer is necessary for the proper design and control of thermomagnetic devices.

Finlayson [1] first discussed thermomagnetic convection and provided a critical stability parameter beyond which this form of convection occurs. Schwab et al. [3] conducted an experimental investigation of the convective instability in a horizontal layer of ferrofluid and characterized the influence of the magnetic Rayleigh number on the Nusselt number. Krakov and Nikiforov [4] addressed the influence of the relative orientation of the temperature gradient and magnetic field on thermomagnetic convection in a square cavity. Yamaguchi et al. [5,6] performed experiments in a square enclosure and characterized the heat transfer in terms of a magnetic Rayleigh number.

However, all of these investigations assumed uniform magnetic fields, which, in most practical heat transfer applications, are not generally realizable. Moreover, the gradient associated with a nonuniform magnetic field is an important component of the thermomagnetic force. Therefore, while these previous studies are significant, they do not fully describe the influence of magnetic

* Corresponding author. Tel.: +1 540 231 3243; fax: +1 540 231 4574.
E-mail address: ikpuri@vt.edu (I.K. Puri).

0017-9310/$ - see front matter © 2005 Elsevier Ltd. All rights reserved.
doi:10.1016/j.ijheatmasstransfer.2005.03.021

Nomenclature

B	magnetic field (T)
C_p	specific heat at constant pressure (kJ/kg K)
D	enclosure height (m)
h	heat transfer coefficient (W/m^2)
H	defined in Eq. (2) (A/m)
$\mathbf{J}_f$	free current density (A/m^2)
k	thermal conductivity (W/mK)
k_B	Boltzmann constant (1.3807×10^{-23} J/K)
m	magnetic moment (strength) per unit length of line dipole (A m)
M	magnetization (A/m)
Nu	Nusselt number (hD/k) (dimensionless)
Pr	Prandtl number (ν/α) (dimensionless)
Ra_m	magnetic Rayleigh number (dimensionless)
t	time (s)
T	temperature (K)
u	x-component of velocity (m/s)
v	y-component of velocity (m/s)
V	velocity vector (m/s)

Greek symbols

α	thermal diffusivity (m^2/s)
β_ρ	fluid compressibility ($-\frac{1}{\rho}\frac{\partial \rho}{\partial T}$) (K^{-1})
χ_0	magnetic susceptibility at reference temperature (dimensionless)
χ_m	magnetic susceptibility at operating temperature (dimensionless)
δ_T	thermal boundary layer thickness (m)
ϕ	coordinate direction
μ	viscosity (Pa s)
λ	Langevin parameter
μ_0	permeability of vacuum (1.257×10^{-6} N/A^2)
ν	kinematic viscosity (m^2/s)
ρ	density (kg/m^3)

field gradients for practically realizable thermomagnetic convection applications. Tangthieng et al. [7] provided a numerical analysis in the presence of a nonuniform field (such as one produced by a permanent magnet), but with two magnetic monopoles.

A few other researchers have considered spatially nonuniform magnetic fields during experimental or numerical investigations, but did not completely represent the variations in those fields [8–12]. In some cases, the field descriptions were inconsistent [7,13] since they were not in accord with the Maxwell's equations of electromagnetism. Consequently, it is not entirely appropriate to employ their correlations between the magnetic field attributes and the resulting heat transfer to design applications. Odenbach [14,15] performed elegant experiments to demonstrate the influence of the thermomagnetic destabilization force in microgravity using an azimuthal magnetic field with a radial gradient (such as one produced by a single current-carrying conductor). Although this magnetic field is realistic, the heat-transfer enhancement as a function of magnetizing current was not characterized in that investigation.

Recently, Ganguly et al. [2,16] addressed these issues by simulating free and forced thermomagnetic convection by considering a two-dimensional magnetic field that is similar to one created by a practical line-source dipole. They have shown that magnetic effects on the corresponding flow are localized. They found that while the addition of dipoles is beneficial for heat transfer, since they create additional recirculation zones, the enhancement in the overall heat transfer depends on the net magnetizing current alone. Wang and Wakayama [17] investigated natural convection with non-conducting and low-conducting diamagnetic fluids with magnetic fields that had different orientations. Tagawa et al. [18] and Kim and Hyun [19] investigated the interaction of thermogravitational and thermomagnetic convection in cubical enclosures under the influence of a magnetic field produced by a pair of electrical coils placed parallel to one pair of faces of the cavity.

Ganguly et al. [16] have shown that the thermomagnetic convection becomes more effective at small length scales, which makes this mode of heat transfer potentially attractive for MEMS applications. However, velocity and temperature measurements at the microscale are challenging. Therefore, some laboratory-scale experiments conducted at larger length scales will need to be appropriately scaled down to extrapolate experimental observations to actual microscale applications. Unfortunately, none of the above work adequately discusses scaling effects for thermomagnetic convection.

2. Formulation

Our configuration is similar to that of Ganguly et al. [16]. Fig. 1(a) presents schematic diagrams of the idealized configurations that we have investigated. The rectangular cavity in Fig. 1(a) extends to infinity (i.e., it has a large depth) in the third dimension such that the flow that develops inside it is two-dimensional. The left hand side vertical wall is maintained at a temperature of T_h while the other vertical wall is an isothermal heat sink at T_c. The upper and lower walls are adiabatic. A line dipole, which provides the external magnetic field, is placed adjacent to the lower wall halfway along the

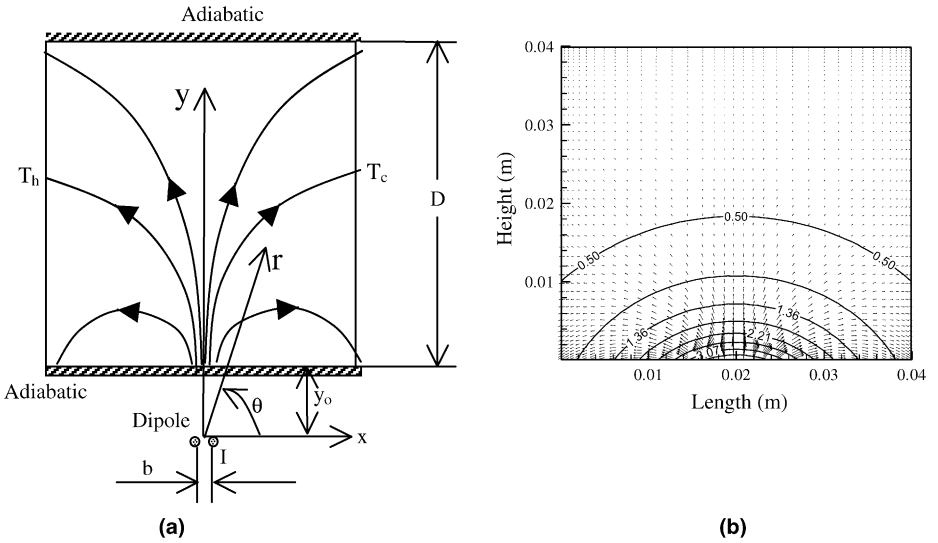

Fig. 1. Schematic diagram of the (a) investigated configuration, and (b) external magnetic field distribution.

enclosure length and at a certain height below its inner surface [2,16]. The resulting field shown in Fig. 1(b) is two-dimensional. It approximates the field produced by an edge-dipole permanent magnet or an electromagnet that is created by a rectangular current-carrying loop of very high aspect ratio (held parallel to the bottom wall of the enclosure). Other realistic fields can also be produced by suitably arranging a number of these line dipoles [20].

The ferrofluid is assumed to be electrically nonconducting so that there is no electromagnetic free current in the flow. We neglect stray electric field effects in the ferrofluid and assume that the magnetic field variation caused by the temperature gradients within the fluid is negligible [21] as compared to the magnetic field gradient itself. This noninductive approximation [22] is valid since it will become evident in the next section that for the ferrofluid properties and magnetic field distribution considered, $|\nabla|\mathbf{H}\| \gg \rho\beta\Delta T/L$. The magnetic field conforms to the Maxwell's relations in static form as

$$\begin{aligned} &\nabla \cdot \mathbf{B} = 0, \\ &\nabla \times \mathbf{H} = \mathbf{0}. \end{aligned} \tag{1}$$

In the above equation, **H** and **B** are related through the expression

$$\mathbf{H} = \frac{1}{\mu_0(1+\chi_m)}\mathbf{B}. \tag{2}$$

The magnetic field inside the fluid due to the line dipole [2,16]:

$$\mathbf{B} = \mu_0(1+\chi_m)m\left[\frac{\sin\phi}{r^2}\mathbf{e_r} - \frac{\cos\phi}{r^2}\mathbf{e_\phi}\right]. \tag{3}$$

The polar coordinate system and the origin of the radius vector r are indicated in Fig. 1(a).

Of the two limiting cases of magnetic fluid behavior discussed by Berkovsky [23], we have considered a fluid of the type for which the total magnetocrystalline anisotropy energy of the nanoparticles is much lower than their thermal fluctuation energy. This implies that the magnetic moment of a domain is not rigidly fixed to the particle body and, consequently, the magnetic field does not influence the particle orientation. Hence, the magnetoviscous effect and consequent anisotropy in other fluid properties are negligible [24]. Since particle rotation (which occurs in a rotational flow-field) does not alter the orientations of their magnetic moments, the overall magnetic moment of the fluid is always aligned with the external magnetic field. Therefore, the fluid is also free from magnetodissipation [25].

Assuming constant thermophysical properties, the governing equations for conservation of mass, momentum and energy are

$$\nabla \cdot \mathbf{V} = 0, \tag{4}$$

$$\rho\left(\frac{\partial \mathbf{V}}{\partial t} + \mathbf{V}\cdot\nabla\mathbf{V}\right) = -\nabla p + \mu\nabla^2\mathbf{V} + (\mathbf{M}\cdot\nabla)\mathbf{B}, \tag{5}$$

$$\rho C_p\left(\frac{\partial T}{\partial t} + \mathbf{V}\cdot\nabla T\right) = k\nabla^2 T. \tag{6}$$

The last term in Eq. (5) represents the Kelvin body force [26,27] (also, please see Appendix A). For small variations in temperature (to which we restrict this analysis), the magnetization of the fluid, **M**, can be expressed in a linearized form as

$$M = M^* + \left(\frac{\partial M}{\partial T}\right)_H (T - T^*) + \left(\frac{\partial M}{\partial H}\right)_T (H - H^*). \quad (7)$$

In the above equation, the quantities with the superscript * denote values at an equilibrium magnetization about which the linearization is performed. Within the range of validity of the linearization, the magnetization vector, **M** and **H** can be related through the state relation [2]

$$\mathbf{M} = \chi_m \mathbf{H}. \quad (8)$$

The susceptibility, χ_m is assumed a function of temperature alone. Again, for a small temperature change, the linearized relation

$$\chi_m = \chi_0[1 + \beta_\rho(T - T^*)]^{-1} \quad (9)$$

is applicable. Hence, the Kelvin body force

$$\begin{aligned}\mathbf{f_M} &= \mu_0 \chi_m \mathbf{H} \cdot \nabla\{(1 + \chi_m)\mathbf{H}\} \\ &= \frac{1}{2}\mu_0 \chi_m (1 + \chi_m)\nabla(\mathbf{H} \cdot \mathbf{H}) + \mu_0 \chi_m (\mathbf{H} \cdot \nabla \chi_m)\mathbf{H}. \quad (10)\end{aligned}$$

Using Eq. (9) and imposing the condition $\beta_\rho(T - T^*) \ll 1$ analogous to the Boussinesq approximation for thermogravitational convection, the following approximations may be used due to the small variations in temperature:

$$\chi_m = \chi_0[1 + \beta_\rho(T - T^*)]^{-1} \approx \chi_0[1 - \beta_\rho(T - T^*)], \quad (11a)$$

$$\begin{aligned}\nabla \chi_m &= -\chi_0[1 + \beta_\rho(T - T^*)]^{-2}\beta_\rho \nabla T \\ &\approx -\frac{\chi_0}{2}[1 - 2\beta_\rho(T - T^*)]\beta_\rho \nabla T, \quad (11b)\end{aligned}$$

and

$$\begin{aligned}\chi_m^2 &= \chi_0^2[1 + \beta_\rho(T - T^*)]^{-2} \\ &\approx \chi_0^2[1 - 2\beta_\rho(T - T^*)]. \quad (11c)\end{aligned}$$

Substituting Eqs. (11a)–(11c) in Eq. (10), we obtain

$$\begin{aligned}\mathbf{f_M} = &\frac{1}{2}\mu_0 \chi_0[1 - \beta_\rho(T - T^*)]\nabla(\mathbf{H} \cdot \mathbf{H}) \\ &+ \frac{1}{2}\mu_0 \chi_0^2[1 - 2\beta_\rho(T - T^*)]\nabla(\mathbf{H} \cdot \mathbf{H}) \\ &+ \mu_0 \chi_0^2 \beta_\rho[1 - 3\beta_\rho(T - T^*)](\mathbf{H} \cdot \nabla T)\mathbf{H}. \quad (12)\end{aligned}$$

Eq. (13) can be further simplified considering the order of magnitude of individual terms. Considering that $\chi_0 \sim O(0.1)$, we can conclude that $\chi_0^2 \leqslant \chi_0$. A representative susceptibility is assumed from the APG E26 ferrofluid data sheet that has also been used by Tynjälä et al. [21]. This enables us to neglect the second term in comparison with the first. Similarly, since $\beta_\rho(T - T^*) \ll 1$, the last term can be simplified to $\mu_0 \chi_0^2 \beta_\rho(\mathbf{H} \cdot \nabla T)\mathbf{H}$. Consequently, the Kelvin body force simplifies into the form

$$\begin{aligned}\mathbf{f_M} = &\frac{1}{2}\mu_0 \chi_0[1 - \beta_\rho(T - T^*)]\nabla(\mathbf{H} \cdot \mathbf{H}) + \mu_0 \chi_0^2 \beta_\rho(\mathbf{H} \cdot \nabla T)\mathbf{H}. \\ &(13)\end{aligned}$$

The first term in Eq. (13) is analogous to the pressure term and has been referred to as "magnetostatic pressure" [2]. Defining an effective pressure as $p^* = p - \frac{\mu_0 \chi_0}{2} H^2$, the momentum equation has the final form

$$\begin{aligned}&\rho \frac{\partial \mathbf{V}}{\partial t} + \rho \mathbf{V} \cdot \nabla \mathbf{V} \\ &\quad = -\nabla p^* + \mu \nabla^2 \mathbf{V} - \frac{1}{2}\mu_0 \chi_0 \beta_\rho (T - T^*)\nabla(\mathbf{H} \cdot \mathbf{H}) \\ &\qquad + \mu_0 \chi_0^2 \beta_\rho (\mathbf{H} \cdot \nabla T)\mathbf{H}. \quad (14)\end{aligned}$$

3. Scaling

Expressing the momentum equations in incompressible form and assuming constant viscosity in terms of scalar components, we obtain the relations

$$\begin{aligned}\frac{\partial u}{\partial t} + u\frac{\partial u}{\partial x} + v\frac{\partial u}{\partial y} = &-\frac{1}{\rho}\frac{\partial p^*}{\partial x} + \nu\left(\frac{\partial^2 u}{\partial x^2} + \frac{\partial^2 u}{\partial y^2}\right) \\ &- \frac{\mu_0 \chi_0}{2\rho}\beta_\rho (T - T^*)\frac{\partial H^2}{\partial x} \\ &+ \frac{\mu_0 \chi_0^2 \beta_\rho}{\rho}\left(H_x \frac{\partial T}{\partial x} + H_y \frac{\partial T}{\partial y}\right)H_x \quad (15)\end{aligned}$$

and

$$\begin{aligned}\frac{\partial v}{\partial t} + u\frac{\partial v}{\partial x} + v\frac{\partial v}{\partial y} = &-\frac{1}{\rho}\frac{\partial p^*}{\partial y} + \nu\left(\frac{\partial^2 v}{\partial x^2} + \frac{\partial^2 v}{\partial y^2}\right) \\ &- \frac{\mu_0 \chi_0}{2\rho}\beta_\rho (T - T^*)\frac{\partial H^2}{\partial y} \\ &+ \frac{\mu_0 \chi_0^2 \beta_\rho}{\rho}\left(H_x \frac{\partial T}{\partial x} + H_y \frac{\partial T}{\partial y}\right)H_y. \quad (16)\end{aligned}$$

Eliminating p^* from Eqs. (15) and (16),

$$\begin{aligned}&\frac{\partial}{\partial y}\left(\frac{\partial u}{\partial t} + u\frac{\partial u}{\partial x} + v\frac{\partial u}{\partial y}\right) - \frac{\partial}{\partial x}\left(\frac{\partial v}{\partial t} + u\frac{\partial v}{\partial x} + v\frac{\partial v}{\partial y}\right) \\ &\quad = \nu\left[\frac{\partial}{\partial y}\left(\frac{\partial^2 u}{\partial x^2} + \frac{\partial^2 u}{\partial y^2}\right) - \frac{\partial}{\partial y}\left(\frac{\partial^2 v}{\partial x^2} + \frac{\partial^2 v}{\partial y^2}\right)\right] \\ &\qquad - \frac{\mu_0 \chi_0}{2\rho}\beta_\rho\left[\frac{\partial H^2}{\partial x}\frac{\partial T}{\partial y} - \frac{\partial H^2}{\partial y}\frac{\partial T}{\partial x}\right] \\ &\qquad + \frac{\mu_0 \chi_0^2 \beta_\rho}{\rho}\left(H_x \frac{\partial T}{\partial x} + H_y \frac{\partial T}{\partial y}\right)\left(\frac{\partial H_x}{\partial y} - \frac{\partial H_y}{\partial x}\right) \\ &\qquad + \frac{\mu_0 \chi_0^2 \beta_\rho}{\rho}\left[H_x \frac{\partial}{\partial y}\left(H_x \frac{\partial T}{\partial x} + H_y \frac{\partial T}{\partial y}\right)\right. \\ &\qquad \left. - H_y \frac{\partial}{\partial x}\left(H_x \frac{\partial T}{\partial x} + H_y \frac{\partial T}{\partial y}\right)\right]. \quad (17)\end{aligned}$$

In Eq. (17), the terms on the left hand side are inertia terms while the first term on the right hand side repre-

sents the viscous effects. The last three terms on the right hand side are various thermomagnetic terms.

Analogous to thermogravitational convection in enclosures, the momentum and energy transfer during strong thermomagnetic convection also occurs through a thin boundary layer near each vertical wall. Consequently, we have adopted the local thickness of the thermal boundary layer $\delta_T(y)$ as the length scale for all variations in x-direction while the height of the enclosure D is used as the length scale for all variations in the y-direction. Following a similar scale analysis for buoyancy-driven convection in enclosures by Bejan [28], the dominant inertia and viscous terms are $\frac{\partial^2 v}{\partial t \partial x} \sim \frac{v}{\delta_T t}$ and $v\frac{\partial^3 v}{\partial x^3} \sim v\frac{v}{\delta_T^3}$.

The scaling of the thermomagnetic terms requires inspection of the configuration. For a magnetic field induced by a line dipole, as reported in Ganguly et al. [2,16], the relevant length scales for variations in H (or H^2) are the width and height of the enclosure. Therefore, H has been scaled with $\frac{m}{D^2}$. For configurations where the variation in H is of the same order as that in H itself, the last two terms in Eq. (17) are clearly much smaller than the first thermomagnetic term. This has also been observed through detailed numerical simulations [16]. However, for configurations where the entire domain is subjected to nearly uniform magnetic fields, the last two terms will determine the order of the thermomagnetic force. Using the above length scales, the dominant thermomagnetic term is of the order of $\frac{\mu_0\chi_0\beta_\rho}{2\rho}\frac{m^2\Delta T}{\delta_T D^5}$. The ratio of the inertia to viscous term is $\sim \delta_T^2/vt$. Since $\delta_T \sim \sqrt{\alpha t}$ [28], this ratio is $\sim Pr^{-1}$. Hence, for fluids with $Pr > 1$, the viscous effects must be balanced with the thermomagnetic terms. This is the range of Pr of interest to us when considering oil-based or water-based ferrofluids.

The balance between viscous and thermomagnetic terms in Eq. (17) yields

$$v \sim \frac{\mu_0\chi_0\beta_\rho\Delta T m^2\delta_T^2}{\rho\nu D^5}. \tag{18}$$

After the initial transient phase, the balance between advection and diffusion in the context of the energy equation implies that

$$v\frac{\Delta T}{D} \sim \alpha\frac{\Delta T}{\delta_T^2}. \tag{19}$$

Substituting Eq. (18) in Eq. (19),

$$\delta_T \sim D\left(\frac{\rho\nu\alpha D^2}{\mu_0\chi_0\beta_\rho m^2\Delta T}\right)^{1/4} \sim DRa_{\mathrm{m}}^{-0.25}, \tag{20}$$

where, as defined by Ganguly et al. [16], the magnetic Rayleigh number

$$Ra_{\mathrm{m}} = \frac{\mu_0\chi_0\beta_\rho m^2\Delta T}{\rho\nu\alpha D^2}. \tag{21}$$

Using the convective heat transfer coefficient, we have the relation $h\Delta T \sim k\frac{\Delta T}{\delta_T}$. Hence, the order of magnitude for the average Nusselt number

$$Nu \sim \frac{hD}{k} \sim \frac{D}{\delta_T} \sim Ra_{\mathrm{m}}^{0.25}. \tag{22}$$

4. Comparison with numerical simulations

The predictions of the scale analysis, described above, were compared with the numerical simulations of Ganguly et al. [16]. The height-averaged Nusselt numbers from that investigation are compared with the predictions of Eq. (22) in Fig. 2. The results are in excellent agreement at higher magnetic Rayleigh numbers ($Ra_{\mathrm{m}} \geqslant 10^6$), but some deviation is observed for lower Rayleigh numbers. This is expected, since at low Rayleigh numbers, the transport is diffusion dominated. In this regime, the scale analysis, which assumes the existence of thin boundary layers, is not strictly applicable. The scale analysis, when extended to low Rayleigh numbers, exaggerates the effect of advection and, consequently, overpredicts the Nusselt number as observed from Fig. 2.

5. Implications for microscale applications

Actual MEMS applications involve length scales of the order of 100 μm or less, while detailed high resolution field measurements involving length scales smaller than ~5 cm are difficult to characterize due to insufficient resolution. Consequently, mesoscale laboratory

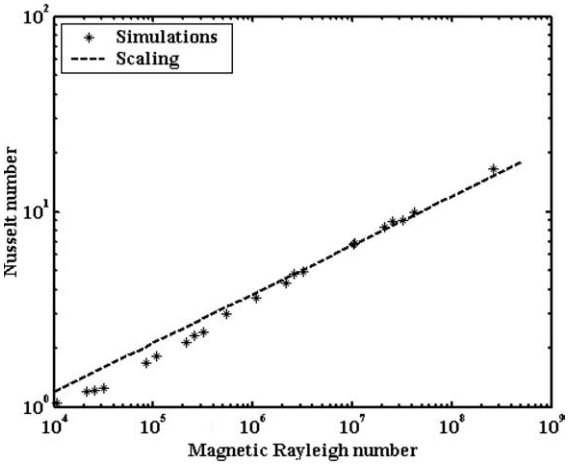

Fig. 2. Comparison of the Nusselt number predicted by the scale analysis presented herein and previous numerical simulations [16].

measurements might need to be scaled down by a factor of 1000 or larger. Considering the nonlinear dependence of the Rayleigh number and the Nusselt number on the length scale, the scaling of heat transfer for these configurations requires careful consideration. Furthermore, since thermomagnetic convection relies on the temperature dependent ferrofluid susceptibility, the magnetic saturation of commercially available magnetic fluids presents a limitation for practical applications (e.g. B_{sat} = 60 mT for an EMG 901 type ferrofluid [29]). Once a ferrofluid is magnetically saturated, strengthening the magnetic field does not enhance thermomagnetic convection. Therefore, the scaling analysis must be suitably modified.

The magnetization of dilute ferrofluids can be expressed by Langevin's equation [30] $M = \varphi M_{sat}(\coth\lambda - 1/\lambda)$, where φ denotes the volume fraction of the solid nanoparticles (≈3%), M_{sat} the saturation magnetization of the bulk material of the particles, $\lambda = \mu_0 m_p H/k_B T$ the Langevin parameter, and m_p the magnetic moment of individual magnetic nanoparticles. Assuming that the Langevin equation for particle magnetization is applicable and that the particles are nearly saturated for $\lambda = 100$ (i.e. when $(\coth\lambda - 1/\lambda) \approx 0.99$), the value of **H** that saturates an EMG 901 ferrofluid is about 1.3×10^6 A/m. Hence, since $H \sim m/D^2$, a combination of m and D values can be used to produce thermomagnetic convection as long as $m/D^2 < 1.3 \times 10^6$. With this upper limit for m/D^2, the value of Ra_m also has an upper bound.

For fixed value of dipole strength m, Eq. (21) shows that Ra_m decreases linearly as D^2 is increased. Thus, a set of parallel curves that relate Ra_m for m_1 = 0.013 A m, m_2 = 1.3 A m and m_3 = 130 A m with varying D are available, as presented in Fig. 3a. Proceeding along each of these curves, a point where m/D^2 exceeds the saturation limit is reached as the length scale is decreased. The area above the curve at this point represents an impracticable space due to the magnetic saturation of the ferrofluid. Eq. (21) also indicates that Ra_m increases linearly with D^2 for fixed values of m/D^2. Thus, $Ra_{m,max}$, which is the maximum achievable value of Ra_m without saturating the ferrofluid, scales with D^2. The different values for $Ra_{m,max}$ for varying m are connected by a curve in Fig. 3a that has a positive slope with respect to D. The results in Fig. 3 use representative values [16] for $\chi_0 = 0.1$, $\beta_\rho = 5.6 \times 10^{-4}$/K, $\rho = 1180$ kg/m^3, $\nu = 5.93 \times 10^{-6}$ m^2/s and $\alpha = 1.19 \times 10^{-7}$ m^2/s.

Eq. (22) establishes a correspondence between Ra_m and Nu. Thus, each of the Ra_m vs. D curves also corresponds to one for Nu vs. D as shown by the set of curves for m_1 = 0.013 A m, m_2 = 1.3 A m and m_3 = 130 A m presented in Fig. 3b. This implies that as the enclosure dimension is reduced, Ra_m and Nu increase for a particular line dipole (characterized by a specific m value) until m/D^2 reaches the maximum permissible value for that ferrofluid. Furthermore, since $Ra_{m,max}$ scales linearly with D^2, the corresponding Nusselt number value Nu_{max} also increases for larger dimensions (shown by the solid line with positive slope in Fig. 3b). For a given dipole strength, if D decreases such that the Nu_{max} limit is reached, a further reduction in length scale reduces the thermomagnetic effect. If the entire ferrofluid inside the enclosure becomes saturated, then Nu equals zero, i.e., there is no convection. Therefore, Fig. 3(b) provides the basis for an optimum enclosure dimension for a particular dipole strength (and vice versa) for which the heat transfer augmentation is maximum. Since saturation progresses from the regions close to the dipole towards those away from it, the corresponding reduction in Nusselt number is gradual. How saturation progresses inside the enclosure and to what extent it influences the Nusselt number is beyond the scope of this analysis.

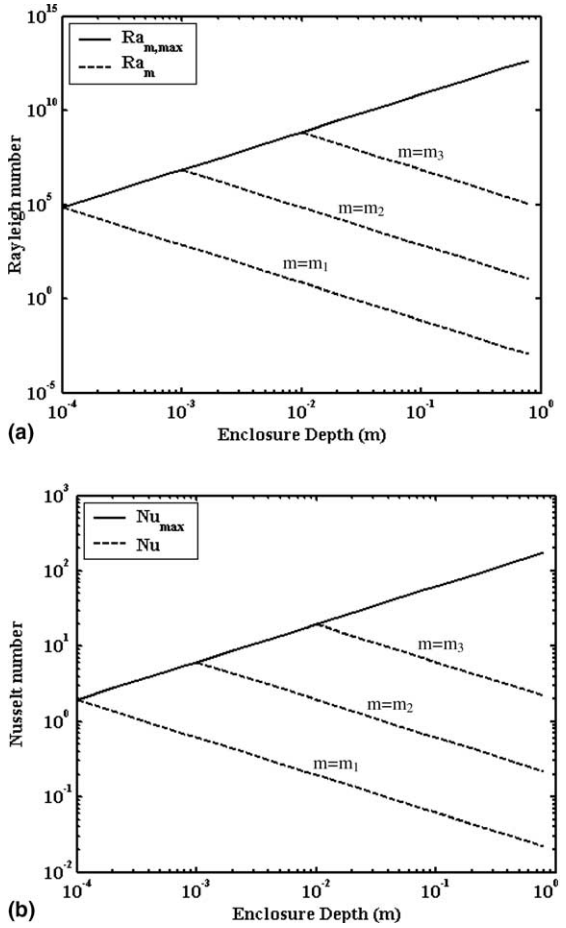

Fig. 3. Variation of the (a) magnetic Rayleigh number and (b) Nusselt number with respect to the enclosure height. The representative dipole strengths are m_1 = 0.013 A m, m_2 = 1.3 A m and m_3 = 130 A m.

6. Conclusions

Thermomagnetic heat transfer in a two-dimensional enclosure filled with a ferrofluid is predicted using a scaling analysis. We have assumed small variations in temperature, so that linearization, analogous to the Boussinesq approximation for thermogravitational convection, becomes possible. The results show that the Nusselt number scales with $Ra_m^{0.25}$, which is in excellent agreement with the predictions of detailed numerical simulations. Imposition of Langevin's relation for a specified value of m leads to an optimum dimension for which the heat transfer rate is maximized.

Appendix A

From an electrodynamics perspective, the Kelvin body force in a magnetic medium occurs due to the magnetization (the bound current) **M** and the magnetic field **B**. A detailed discussion regarding the magnetic body force term can be found in Ref. [26], where the expression of magnetic body force density is written in the form

$$\mathbf{F} = \mu_0(\mathbf{M}\cdot\nabla)\mathbf{H} + \mu_0\mathbf{J}_f \times \mathbf{H} + \nabla\left(\frac{\mu_0}{2}\mathbf{M}\cdot\mathbf{M}\right). \qquad (A.1)$$

In this case, the free current density $\mathbf{J}_f$ is zero in the ferrofluid. The last term in Eq. (A.1) vanishes if the control surface encloses the magnetizable body completely. Consequently, the expression for the magnetic body force is consistent with that used in Refs. [1] and [4]. The same expression is also recovered when one considers the total magnetic body force integrated over the surface of the magnetizable body (i.e., for the case when the control surface encloses the entire body and passes through a region where $\mathbf{M} = 0$). However, our analysis considered an arbitrary control volume which can hypothetically be fully submerged within the ferrofluid. Thus, the last term in Eq. (A.1) is not necessarily zero and the relevant expression for the body force density is that described by Eq. (5). This is also in accord with the expression used in Ref. [27].

References

[1] B.A. Finlayson, Convective instability of ferromagnetic fluids, J. Fluid Mech. 40 (1970) 753–767.

[2] R. Ganguly, S. Sen, I.K. Puri, Heat transfer augmentation using a magnetic fluid under the influence of a line dipole, J. Magn. Magn. Mater. 271 (2004) 63–73.

[3] L. Schwab, U. Hildebrandt, K. Stierstadt, Magnetic Bénard convection, J. Magn. Magn. Mater. 39 (1983) 113–114.

[4] M.S. Krakov, I.V. Nikiforov, To the influence of uniform magnetic field on thermomagnetic convection in square cavity, J. Magn. Magn. Mater. 252 (2002) 209–211.

[5] H. Yamaguchi, I. Kobori, Y. Uehata, K. Shimada, Natural convection of magnetic fluid in a rectangular box, J. Magn. Magn. Mater. 201 (1999) 264–267.

[6] H. Yamaguchi, I. Kobori, Y. Uehata, Natural convection of magnetic fluid in a rectangular box, J. Thermophys. Heat Transfer 13 (1999) 501–507.

[7] C. Tangthieng, B.A. Finlayson, J. Maulbetsch, T. Cader, Finite element model of magnetoconvection of a ferrofluid, J. Magn. Magn. Mater. 201 (1999) 252–255.

[8] T. Sawada, H. Kikura, A. Saito, T. Tanahashi, Natural convection of a magnetic fluid in concentric horizontal annuli under nonuniform magnetic fields, Expt. Thermal Fluid Sci. 7 (1993) 212–220.

[9] S.M. Snyder, T. Cader, B.A. Finlayson, Finite element model of magnetoconvection of a ferrofluid, J. Magn. Magn. Mater. 262 (2003) 269–279.

[10] H. Yamaguchi, Z. Zhang, S. Shuchi, K. Shimada, Heat transfer characteristics of magnetic fluid in a partitioned rectangular box, J. Magn. Magn. Mater. 252 (2002) 203–205.

[11] S. Kamiyama, K. Ueno, Y. Yokota, Numerical analysis of unsteady gas–liquid two-phase flow of magnetic fluid, J. Magn. Magn. Mater. 201 (1999) 271–275.

[12] K. Nakatsuka, B. Jeyadevan, S. Nevebu, H. Koganezawa, The magnetic fluid for heat transfer applications, J. Magn. Magn. Mater. 252 (2002) 360–362.

[13] H. Yamaguchi, I. Kobori, N. Kobayashi, Numerical study of flow state for a magnetic fluid heat transport device, J. Magn. Magn. Mater. 201 (1999) 260–263.

[14] S. Odenbach, Microgravity experiments on thermomagnetic convection in magnetic fluids, J. Magn. Magn. Mater. 149 (1995) 155–157.

[15] S. Odenbach, Sounding rocket and drop tower experiments on thermomagnetic convection in magnetic fluids, Adv. Space Res. 16 (7) (1995) 99–104.

[16] R. Ganguly, S. Sen, I.K. Puri, Thermomagnetic convection in a square enclosure using a line dipole, Phys. Fluids 16 (7) (2004) 2228–2236.

[17] L.B. Wang, N.I. Wakayama, Control of natural convection in non- and low-conducting diamagnetic fluids in a cubical enclosure using inhomogeneous magnetic fields with different directions, Chem. Engng. Sci. 57 (2002) 1867–1876.

[18] T. Tagawa, R. Shigemitsu, H. Ozoe, Magnetizing force modeled and numerically solved for natural convection in a cubic enclosure: effect of the direction of the magnetic field, Int. J. Heat Mass Transfer 45 (2002) 267–277.

[19] K.H. Kim, J.M. Hyun, Buoyant convection in a cubical enclosure under time-periodic magnetizing force, Int. J. Heat Mass Transfer 47 (2004) 5211–5218.

[20] D.J. Griffiths, Introduction to Electrodynamics, third ed., Prentice Hall Inc., 2002.

[21] T. Tynjälä, A. Hajiloo, W. Polashenski Jr., P. Zamankhan, Magnetodissipation in ferrofluids, J. Magn. Magn. Mater. 252 (2002) 123–125.

[22] B. Berkovsky, Thermomagnetic convection, in: V. Bashtovoy (Ed.), Magnetic Fluids and Applications Handbook, Begell House, Inc, 1996, pp. 549–577.

[23] B. Berkovsky, Some aspects of theoretical modeling of thermomechanics of magnetic fluids, in: B. Berkovsky (Ed.), Proc. of the Int. Adv. Course and Workshop on

Thermomechanics of Magnetic Fluids, Hemisphere Publishing Corporation, pp. 149–157.
[24] M.I. Shliomis, V.I. Stepanov, Rotational viscosity of magnetic fluids—contribution of the Brownian and Neél relaxational processes, J. Magn. Magn. Mater. 122 (1993) 196–199.
[25] H.W. Müller, A. Engel, Dissipation in ferrofluids: mesoscopic versus hydrodynamic theory, Phys. Rev. E 60 (6) (1999) 7001–7009.
[26] M. Zahn, Introduction to Electromagnetic Field Theory: a Problem Solving Approach, John Willey and Sons, Inc., New York, 1979, Chapter 5, p. 369, Eq. (9).
[27] D. Gignoux, J.C. Peuzin, Magnetistatics, in: É. du T. de Lacheisserie, D. Gignoux, M. Schlenker (Eds.), Magnetism I—Fundamentals, Kluwer Academic Publishers, 2002, pp. 19–78.
[28] A. Bejan, Convection Heat Transfer, first ed., Wiley, New York, 1984.
[29] J. Weilepp, H.R. Brand, Competition between the Benard–Marangoni and the Rosensweig instabilities in magnetic fluids, J. Phys. II France 6 (1996) 419–441.
[30] A. Lange, Kelvin force in a layer of magnetic fluid, J. Magn. Magn. Mater. 241 (2002) 327–329.